

Current sensor based on an atomic magnetometer for DC application

Guozhu Li (李国祝)¹, Qing Xin (辛青)^{1,*}, Xuxing Geng (耿旭兴)², Zhi Liang (梁植)², Shangqing Liang (梁尚清)¹, Guangming Huang (黄光明)², Gaoxiang Li (李高翔)², and Guoqing Yang (杨国卿)^{1,**}

¹College of Electronics and Information, Hangzhou Dianzi University, Hangzhou 310018, China

²College of Physics, Huazhong Normal University, Wuhan 430079, China

*Corresponding author: xinqing@hdu.edu.cn; **corresponding author: gqyang@hdu.edu.cn

Received November 2, 2019; accepted November 28, 2019; posted online February 21, 2020

A DC current sensor based on an optically pumped atomic magnetometer is proposed. It has a high linearity in a wide operation range, since the magnetometer measures the absolute magnitude of the magnetic field produced by the current to be measured. The current sensor exhibits a high accuracy with a non-moment solenoid and magnetic shielding to suppress the influence from the environment. The absolute error of the measured current is below 0.08 mA when the range is from 7.5 mA to 750 mA. The relative error is 5.54×10^{-5} at 750 mA.

Keywords: current sensor; atomic magnetometer; high accuracy.

doi: 10.3788/COL202018.031202.

Precision DC current sensing techniques are required by scientific studies and industrial applications. Current measurements with high accuracy are usually applied to current sources in fundamental research. Currents were controlled with feedback systems to produce stable magnetic fields in the Watt balance experiment, whose purpose was to realize the electronic kilogram^[1]. Accurate DC current measurement can be used to evaluate current generators at the picoampere level for the calibration of other electrical instruments^[2]. Precise current measurement can be applied to keep the magnetic fields in the large hadron collider consistent^[3]. DC current measurement is also very important and widely used in the applications for power management, industrial control, and conditions monitoring. The DC current component in power grids induced by geomagnetic activities is monitored to prevent the saturation of transformers^[4]. Sensors capable of measuring DC current up to a kiloampere are desirable for electrowinning industries^[5]. Besides accuracy and stability, linearity is an important parameter in automotive applications^[6]. However, it is difficult to maintain high accuracy in a wide operating range. Thermal drift and nonlinearity of the material in a high field are the main reasons to degrade the linearity of current sensors.

Current sensing techniques with magnetic field sensors have attracted wide attention, with emphasis on the study of high accuracy and linearity. Several compensation methods have been proposed. Thermal drift can be compensated with temperature monitoring in a magnetoresistive current sensor^[7]. Differential structure has been used to protect current sensors from external magnetic fields for high accuracy^[8,9]. The closed-loop configuration with a magnetic core and a feedback winding in a fluxgate current sensor can improve the sensitivity and eliminate the offset and drift related to temperature^[10]. Another effective approach is utilizing magnetometers that have a

low thermal drift and nonlinearity and are suitable for a highly accurate current sensor. Atom ensembles can be used to produce a chip-scale high accuracy sensor^[11,12]. Current sensors with atomic magnetometers have been articulated for a broad range of *in situ* calibration purposes^[13]. The strength of the magnetic field B produced by the current to be measured is related to the Larmor precession frequency f_L by the atomic g-factor^[14]. Since most g-factors can be traceable to about 10^{-7} ^[15], an atomic magnetometer can be used to accurately define a magnetic field^[16]. It is expected to have uncertainties in the range of parts in 10^6 . The magnetic resonance spectrum for magnetometers can work in a wide magnetic field range and exhibit a sharp peak when it is in resonance^[17,18]. Atomic magnetometers can be used for current sensors with high accuracy and linearity.

In this Letter, we propose a new current sensor based on an optically pumped atomic magnetometer. The current sensor has high linearity in a wide range because the atomic magnetometer is a kind of absolute magnetometer using the fixed atomic g-factor. To achieve high accuracy, we design a non-moment solenoid to produce a magnetic field that has a stable relationship with the current to be measured. Finally, we experimentally demonstrate a DC current sensor with a high accuracy and linearity.

A schematic diagram of the proposed current sensor is shown in Fig. 1. The M_z type optically pumped atomic magnetometer is applied in the current sensor^[18]. An 895 nm laser diode is used as a light source that is locked to the cesium D_1 line $F_g = 4$ to $F_e = 3$ transition with saturated absorption spectroscopy. The light from the laser diode is collimated and converted to circular polarization with a lens and a quarter-wave plate (not drawn in Fig. 1). The resonant light and a resonant radio frequency (RF) field excite the cesium atoms in the magnetic field, which causes magnetic resonance. The signal is detected by a

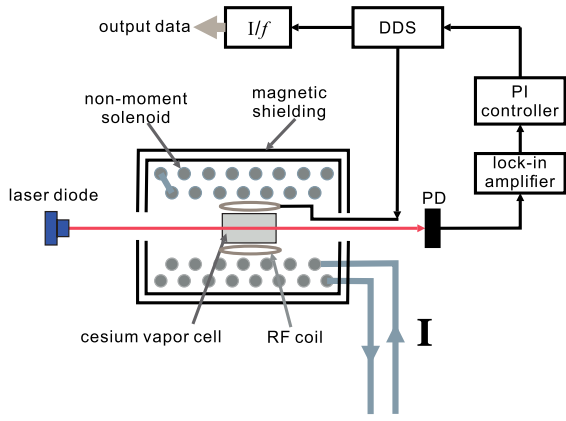


Fig. 1. Schematic diagram of the proposed current sensor. I : current to be measured; PD: photodiode; PI: proportional-integral; DDS: direct digital synthesis; RF: radio frequency; I/f : Larmor frequency to I data converter.

photodiode and sent to the lock-in amplifier. The output signal is a differential form of the Lorentzian magnetic resonance curve that is used to lock the RF field at the resonant point with a proportional-integral (PI) controller. When the system works, the frequency of the direct digital synthesis (DDS) equals the Larmor precession frequency of the cesium atoms. The current data is then obtained with a conversion program.

A fixed relation between the output of the atomic magnetometer and the current to be measured is established as follows. The cesium atoms with 50 Torr (1 Torr = 133.32 Pa) N_2 gas are filled in a $\varnothing 20$ mm \times 30 mm vapor cell that senses the magnetic field produced by a non-moment solenoid, which consists of two coaxial finite length coils with opposite directions of current. The vapor cell is placed in the middle of the solenoid with a holder. Then the magnetic field has a fixed relationship with the current to be measured. The magnetic field B of one finite length solenoid is

$$B = \mu_0 n I \left[\frac{d+x}{\sqrt{R^2 + (d+x)^2}} + \frac{d-x}{\sqrt{R^2 + (d-x)^2}} \right], \quad (1)$$

where μ_0 is the permeability in vacuum, n is the winding density, d is half of the full length of the solenoid, R is the radius of the solenoid, and x is the distance from the middle point of the solenoid. The parameters of the non-moment solenoid satisfy the relations

$$R_1^2 + d_1^2 = R_2^2 + d_2^2, \quad (2)$$

$$R_1^2 N_1 = R_2^2 N_2, \quad (3)$$

where N_1 and N_2 are the winding numbers. Equation (2) makes the solenoid generate a uniform magnetic field. Equation (3) makes the total magnetic moment of the solenoid zero. Under these conditions, the magnetic field in the solenoid has a high uniformity and the distribution is not affected by magnetic shielding. The environmental

magnetic noise is suppressed by magnetic shielding. The optically pumped atomic magnetometer has a high performance and a small nonlinear Zeeman shift when the magnetic field is below 100,000 nT. To achieve a high sensitivity and accuracy simultaneously if the measured current is below 1 A, we use Eqs. (1)–(3) to obtain the parameters. The radius of the outer coil is 75 mm while that of the inner coil is 65 mm. The length of the solenoid is 500 mm and the winding numbers are 135.5 and 180.5 for N_1 and N_2 , respectively. The coefficient of the non-moment solenoid is then 108.6 nT/mA.

We make the non-moment solenoid with the above parameters and simulate the distribution of the magnetic field with ANSYS. The result is shown in Fig. 2. The relative deviation in the center area ($\varnothing 50$ mm \times 50 mm) is less than 10^{-5} . That means the accuracy will not be affected by the gradient of the magnetic field.

To evaluate the performance of the current sensor, we use a Keysight B2962A as the current source. It is calibrated by a current standard and the relative error is below 10^{-5} when the output is 1 A. We set several test points from 7.5 mA to 750 mA. Each point is the average value of ten minutes data. The amplitude of the magnetic field B is calculated based on the Zeeman effect. The nonlinear Zeeman effect is considered for high accuracy^[19]. The calculated current is $B/108.6$.

The current sensor can exhibit high linearity in a wide operation range, which benefits from the optically pumped atomic magnetometer. Since it is a kind of absolute magnetometer, the atomic magnetometer makes the current sensor have an approximate low absolute error in the whole operation range. Figure 3 shows the measured magnetic field and calculated current versus the actual current.

The absolute error of the measured current is below 0.08 mA when the range is from 7.5 mA to 750 mA, as shown in Fig. 4. The absolute accuracy of the optically

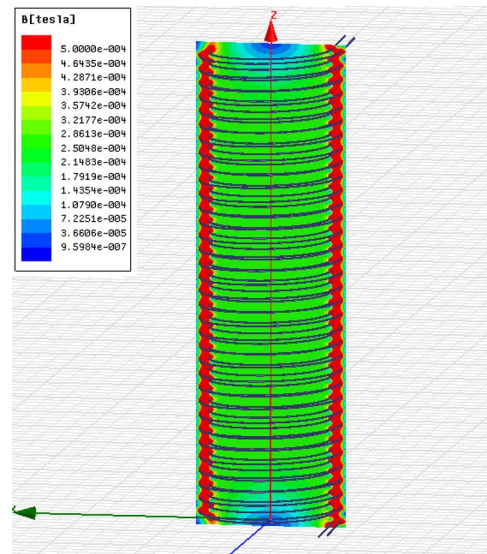


Fig. 2. Distribution of the magnetic field in the solenoid, which is simulated with ANSYS. The current is 1 A.

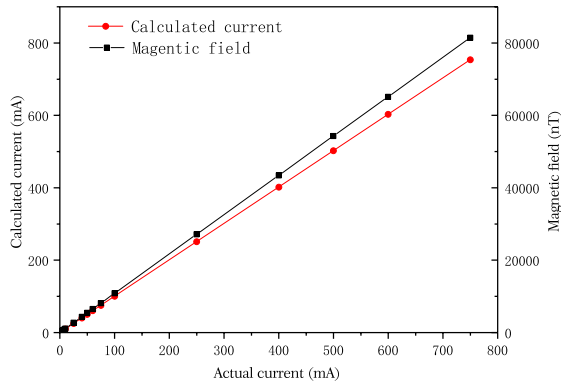


Fig. 3. Measured magnetic field (square) and calculated current (dot) versus actual current.

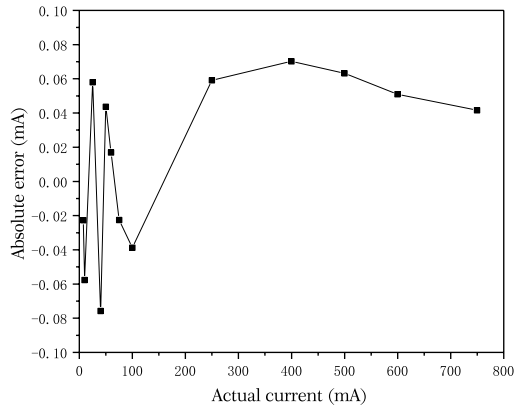


Fig. 4. Absolute error versus actual current.

pumped atomic magnetometer is usually at the nT level. The equivalent accuracy of the magnetic field measurement in the current sensor is better than 8.7 nT. The absolute error of the commercial current source, the actual magnetic field distribution in the non-moment solenoid, and the absolute accuracy of the magnetometer would contribute to the performance of the prototype of the current sensor. The maximum absolute error of the current is about $750 \text{ mA} \times 10^{-5} = 0.0075 \text{ mA}$, the influence of which is neglectable here. The absolute error derived from the solenoid is mainly induced by the manufacture accuracy. The length tolerance is $\pm 0.01 \text{ mm}$, the radius tolerance is $\pm 0.01 \text{ mm}$, and the assembly tolerance is $\pm 0.05 \text{ mm}$. We simulate the distribution of the magnetic field with ANSYS. The maximum absolute error of the coefficient of the non-moment solenoid is 0.004 nT/mA. Therefore, the maximum absolute error derived from the solenoid in our experiment is about 0.03 mA when the current is 750 mA. Then the absolute error derived from the magnetometer is larger than 0.05 mA, which means that the absolute error of the magnetometer is larger than 5.4 nT. The absolute accuracy of an optically pumped atomic magnetometer is mainly affected by the linewidth of the magnetic resonance, the relative phase of the lock-in amplifier module, and the deviation of reference voltage in

the closed-loop circuit. The absolute accuracy of a high-performance commercial cesium optically pumped atomic magnetometer is 2.5 nT. So the absolute error of the current sensor derived from the magnetometer can be reduced to 0.025 mA. Obviously, the absolute error of the current sensor is limited by the atomic magnetometer. The performance can be improved by applying an M_Z -type potassium optically pumped atomic magnetometer with absolute accuracy of 0.1 nT^[20]. The corresponding contribution to the absolute error of the current sensor is 0.92 μA . If the absolute error of the current is much lower than 0.92 μA , the current sensor can be well calibrated and then the absolute error is 0.92 μA . Also, we can improve the absolute accuracy by increasing the coefficient of the non-moment solenoid, but the operation range will be reduced.

Since the absolute error does not have significant change, the relative error becomes smaller as the actual current increases, as shown in Fig. 5. The relative error is 5.54×10^{-5} at 750 mA. Furthermore, we evaluate the performance of the current sensor with an Allan deviation, as shown in Fig. 6. The current is 100 mA. The sampling

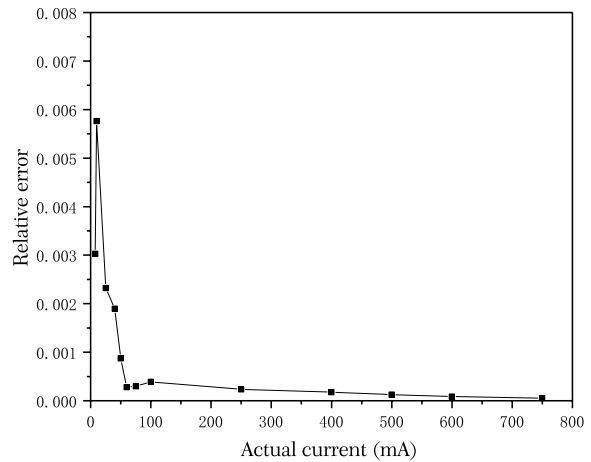


Fig. 5. Relative error versus actual current.

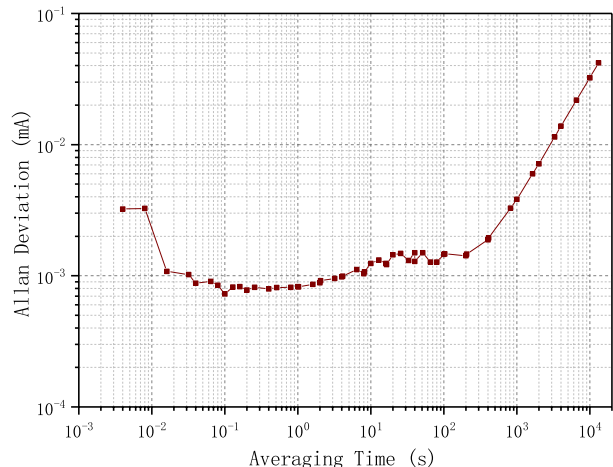


Fig. 6. Allan variance of the current sensor data.

rate is 250 Hz, and the output of the current sensor is recorded for 24 h. The short-term stability is below 1 μA with averaging time from 0.04 to 2 s. The value related to the averaging time of ten minutes is consistent with the data in Fig. 4.

In conclusion, we demonstrate a high accuracy and linearity DC current sensor based on an optically pumped atomic magnetometer. The absolute error of the measured current is below 0.08 mA when the range is from 7.5 mA to 750 mA. The relative error is 5.54×10^{-5} at 750 mA.

References

1. R. Steiner, D. Newell, and E. Williams, *J. Res. Natl. Inst. Stand. Technol.* **110**, 1 (2005).
2. B. Ehtesham, P. S. Bist, and T. John, *MAPAN* **32**, 17 (2017).
3. M. C. Bastos, G. Fernqvist, G. Hudson, J. Pett, A. Cantone, F. Power, A. Saab, B. Halvarsson, and J. Pickering, *IEEE Instrum. Meas. Mag.* **17**, 66 (2014).
4. P. Ripka, K. Draxler, and R. Styblikova, *IEEE Trans. Magn.* **49**, 73 (2013).
5. E. Fiorucci and G. Bucci, *IEEE Trans. Instrum. Meas.* **62**, 845 (2013).
6. A. Patel and M. Ferdowsi, *IEEE Trans. Veh. Technol.* **58**, 4108 (2009).
7. J. S. Moreno, D. R. Munoz, S. Cardoso, S. C. Berga, A. E. N. Anton, and P. J. P. Freitas, *Sensors* **11**, 2447 (2011).
8. S. Lee, S. Hong, W. Park, W. Kim, J. Lee, K. Shin, C. Kim, and D. Lee, *Sensors* **18**, 2231 (2018).
9. M. Zhang and S. W. Or, *Sensors* **18**, 588 (2018).
10. X. Yang, Y. Li, W. Zheng, W. Guo, Y. Wang, and R. Yan, *IEEE Trans. Magn.* **51**, 4002804 (2015).
11. Y. Pan, W. Liao, H. Wang, Y. Yao, J. Cai, and J. Qu, *Chin. Opt. Lett.* **17**, 060201 (2019).
12. L. Zhang, W. Zhang, S. Zhang, and S. Yan, *Chin. Opt. Lett.* **17**, 100201 (2019).
13. J. Kitching, E. A. Donley, S. Knappe, M. Hummon, A. T. Dellis, J. Sherman, K. Srinivasan, V. A. Aksyuk, Q. Li, D. Westly, B. Roxworthy, and A. Lal, *J. Phys. Conf. Ser.* **723**, 012056 (2016).
14. D. Budker and M. Romalis, *Nat. Phys.* **3**, 227 (2007).
15. W. D. Phillips, W. E. Cooke, and D. Kleppner, *Phys. Rev. Lett.* **35**, 1619 (1975).
16. S. Liang, G. Yang, Y. Xu, Q. Lin, Z. Liu, and Z. Chen, *Opt. Express* **22**, 6837 (2014).
17. D. Budker and D. F. J. Kimball, *Optical Magnetometry* (Cambridge University Press, 2013).
18. G. Yang, H. Zhang, X. Geng, S. Liang, Y. Zhu, J. Mao, G. Huang, and G. Li, *Opt. Express* **26**, 30313 (2018).
19. D. A. Steck, <https://steck.us/alkalidata/cesiumnumbers.1.6.pdf> (1998).
20. E. Pulz, K.-H. Jackel, and H.-J. Linthe, *Meas. Sci. Technol.* **10**, 1025 (1999).